

Current Biology

The genome of *Geosiphon pyriformis* reveals ancestral traits linked to the emergence of the arbuscular mycorrhizal symbiosis

Highlights

- High content of transposable elements are identified in the genome of *G. pyriformis*
- Sugar thiamine metabolisms and fatty acid biosynthesis are absent in *G. pyriformis*
- Evidence of horizontal gene transfers between *Geosiphon* and *Nostoc* is found
- Conserved MAT locus and meiosis-specific genes are present in this species

Authors

Mathu Malar C, Manuela Krüger, Claudia Krüger, ..., Christophe Roux, Pierre-Marc Delaux, Nicolas Corradi

Correspondence

mmadhubioinfo@gmail.com (M.M.C.),
ncorradi@uottawa.ca (N.C.)

In Brief

Malar C et al. sequenced the genome of the AMF *Geosiphon pyriformis*, a species that can form endosymbiosis with a cyanobacterium. The *G. pyriformis* genome carries all the hallmarks of AMF obligate plant biotrophy. Our findings indicate that the mechanisms involved in arbuscular mycorrhizal symbiosis appeared prior to the emergence of Glomeromycotina.

Report

The genome of *Geosiphon pyriformis* reveals ancestral traits linked to the emergence of the arbuscular mycorrhizal symbiosis

Mathu Malar C,^{1,8,9,*} Manuela Krüger,^{2,3,8} Claudia Krüger,^{2,3,8} Yan Wang,^{4,5} Jason E. Stajich,⁶ Jean Keller,⁷ Eric C.H. Chen,¹ Gokalp Yildirim,¹ Matthew Villeneuve-Laroche,¹ Christophe Roux,⁷ Pierre-Marc Delaux,⁷ and Nicolas Corradi^{1,10,11,*}

¹Department of Biology, University of Ottawa, Ottawa, ON, Canada

²Institute of Botany, The Czech Academy of Sciences, Průhonice, Czech Republic

³Institute of Experimental Botany, The Czech Academy of Science, Prague, Czech Republic

⁴Department of Biological Sciences, University of Toronto Scarborough, Toronto, ON, Canada

⁵Department of Ecology and Evolutionary Biology, University of Toronto, Toronto, ON, Canada

⁶Department of Microbiology & Plant Pathology and Institute for Integrative Genome Biology, University of California, Riverside, Riverside, CA, USA

⁷Laboratoire de Recherche en Sciences Végétales, Université de Toulouse, UPS, CNRS 24 Chemin de Borde Rouge-Auzeville, Castanet-Tolosan, France

⁸These authors contributed equally

⁹Twitter: @madhubioinfo

¹⁰Twitter: @Blunt_Microbe

¹¹Lead contact

*Correspondence: mmadhubioinfo@gmail.com (M.M.C.), ncorradi@uottawa.ca (N.C.)

<https://doi.org/10.1016/j.cub.2021.01.058>

SUMMARY

Arbuscular mycorrhizal fungi (AMF) (subphylum Glomeromycotina)¹ are among the most prominent symbionts and form the Arbuscular Mycorrhizal symbiosis (AMS) with over 70% of known land plants.^{2,3} AMS allows plants to efficiently acquire poorly soluble soil nutrients⁴ and AMF to receive photosynthetically fixed carbohydrates. This plant-fungus symbiosis dates back more than 400 million years⁵ and is thought to be one of the key innovations that allowed the colonization of lands by plants.⁶ Genomic and genetic analyses of diverse plant species started to reveal the molecular mechanisms that allowed the evolution of this symbiosis on the host side, but how and when AMS abilities emerged in AMF remain elusive. Comparative phylogenomics could be used to understand the evolution of AMS.^{7,8} However, the availability of genome data covering basal AMF phylogenetic nodes (Archaeosporales, Paraglomerales) is presently based on fragmentary protein coding datasets.⁹ *Geosiphon pyriformis* (Archaeosporales) is the only fungus known to produce endosymbiosis with nitrogen-fixing cyanobacteria (*Nostoc punctiforme*) presumably representing the ancestral AMF state.^{10–12} Unlike other AMF, it forms long fungal cells (“bladders”) that enclose cyanobacteria. Once in the bladder, the cyanobacteria are photosynthetically active and fix nitrogen, receiving inorganic nutrients and water from the fungus. Arguably, *G. pyriformis* represents an ideal candidate to investigate the origin of AMS and the emergence of a unique endosymbiosis. Here, we aimed to advance knowledge in these questions by sequencing the genome of *G. pyriformis*, using a re-discovered isolate.

RESULTS

General genome characteristics of *Geosiphon pyriformis*

The only known culture of *G. pyriformis* was lost over a decade ago. In an attempt to rediscover *G. pyriformis*, we searched and identified symbiotic bladders of the *G. pyriformis*-*N. punctiforme* symbiosis (Figure 1) at the only known stable habitat of this species in the Spessart Mountains near the village of Bieber in Germany.¹³

Upon cultivation, we extracted DNA and RNA from active bladders. Total DNA was subjected to 5 kb mate-pair and

125 bp paired-end Illumina sequencing, producing, respectively, 47 and 81 million 125 bp paired ends and 5 kb mate-pairs reads. *G. pyriformis* reads were identified using a read binning approach recently implemented to assemble the genome of *Diversispora epigea*,¹⁵ and upon identification these were assembled into a 129 MB assembly and 795 scaffolds with an average read coverage of 118X. In parallel, total RNA was subjected to 150 bp paired-end Illumina sequencing. The resulting RNA sequencing (RNA-seq) reads were mapped onto the *G. pyriformis* genome assembly using STAR¹⁶ and used for genome annotation after implementing RepeatMasker.¹⁷ This procedure identified of 24,195 genes in *G. pyriformis*, resulting

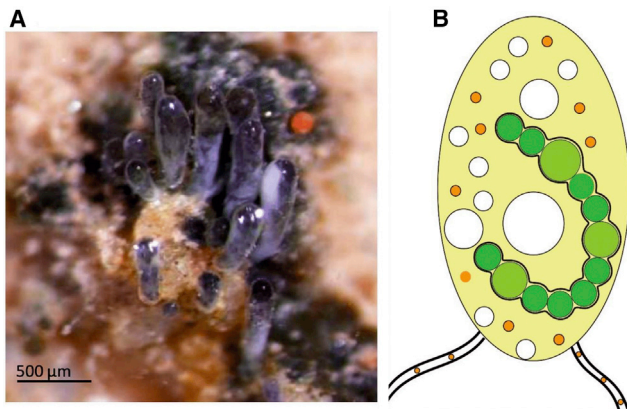


Figure 1. Morphology of symbiotic bladders of *Geosiphon pyriformis* and *Nostoc punctiforme*

(A) Image of *G. pyriformis* bladders in soil from its natural habitat in the Spessart mountains.

(B) Schematic representation of *G. pyriformis* bladders containing *Nostoc* cells (based on Kluge, 2002¹⁴). *Nostoc* cells are shown in dark green, and heterocysts (differentiated cell that carries out nitrogen fixation) are shown in light green. Bladders contain *G. pyriformis* nuclei (orange) and several vacuoles (white). Aseptate hyphae reach out and extend from the bladders.

in a BUSCO gene repertoire completeness of 96.2% (3.1% complete duplicated). The gene counts, estimated genome size, and genome statistics are all similar to those of model AMF species^{18,19} and are indicative of high genome completeness (Table 1; see figure of “K-mer distribution of filtered Illumina genomic reads of *G. pyriformis*” in Data S1 and see table of “Genome completeness using Busco” in Data S1). SignalP showed that, among all the genes identified in *G. pyriformis*, 365 represent putative secreted proteins (see table of “Secretome proteins from genomes” in Data S1), and 27% of these are candidate effectors (see table of “Effector prediction on *G. Pyriformis* genome” in Data S1). We also identified 19 putative secreted CAZymes in *G. pyriformis*, in line with numbers found in other AMF species (Tables S1 and S2).

AMF genomes carry a substantial fraction of transposable elements (TEs),^{19–22} and we found that *G. pyriformis* has undergone similar TE expansions. The expansion of Gypsy transposable elements in *G. pyriformis* is evident in comparison to all other AMF genomes (Figure 2). With regards to TEs, we found no evidence that *G. pyriformis* (see figure of “Heatmap showing evidence for a “one-speed genome” in *Geosiphon Pyriformis*” in Data S1) carries a two-speed genome.²³ Two-speed genomes are characterized by the presence of TE-poor and gene-dense regions that are clearly separate from others that contain rapidly evolving genomic regions that usually carry fewer genes, abundant TEs, and other repeat elements.^{23,24}

Using genome data and single nucleus data, it was recently shown that AMF carry two genome organizations—i.e., homokaryotic (co-existing nuclei carry one parental haploid genotype) or heterokaryotic (two parental genotypes co-exist in the mycelium).^{22,25–27} Mapping reads onto the *G. pyriformis* genome revealed reduced levels of polymorphism (0.5 SNP/Kb) and allelic frequencies suggesting that this species carries low nuclear diversity and is likely homokaryotic (see figure of “Genome

wide allele frequency of *G. Pyriformis* shows it is a homokaryon” in Data S1).

Placement of *G. pyriformis* based on phylogenomics

The *G. pyriformis* genome annotation was used to identify the phylogenetic placement of this species using amino-acid sequences. In this case, we used a set of 434 conserved fungal single-copy genes (data available at 10.5281/zenodo.1413687) to construct a phylogenetic tree of the fungal kingdom. Phylogenomics supports the monophyly of Glomeromycotina and its close relationship with Mortierellomycotina within the phylum Mucoromycota¹ (Figure 3). Within Glomeromycotina, *G. pyriformis* groups with *Ambispora leptoticha* and *Paraglomus occultum*, which diverged around 287 MYA (Figure S1). This clade is distinct from more diverged nodes that contain sequenced representatives from Glomerales and Diversisporales.²⁸ The current placement of *G. pyriformis* as a sister lineage to *A. leptoticha* and *P. occultum* has full statistical support and is favored by 73% of the gene sequences we used. Alternative topologies that place, for example, *G. pyriformis* at a basal node to all AMF (Alt-T1; Figure S2, see table of “Results of alternative tree topology test for phylogenetic tree” in Data S1) or as being associated with Glomerales or Diversisporales (Alt-T2 and Alt-T3; Figure S2, see table of “Results of alternative tree topology test for phylogenetic tree” in Data S1) were all rejected significantly using statistical tests implemented in IQ-TREE, including the KH, SH, ELW, and AU tests (see table of “Results of alternative tree topology test for phylogenetic tree” in Data S1).

The genome of *Geosiphon pyriformis* uncovers shared gene features in the Glomeromycotina

Phylogenomics revealed that *G. pyriformis* is a member of a clade that diverged early from the lineage encompassing the already sampled Diversisporales and Glomerales. As such, the *G. pyriformis* genome fills the gap in the genomic coverage of major AMF phylogenetic clades. With this data in hand, we first searched for genetic features that arose in the MRCAs of all Glomeromycotina by comparing orthogroups from five available AMF genomes and four other members of the Mucoromycota as outgroups using OrthoFinder.²⁹ This analysis identified 661 gains and 344 losses that occurred before the divergence of the Glomeromycotina (Table S3; see table of “Orthogroups lost in the MRCAs of Glomeromycotina” in Data S1).

Among the 344 orthogroups classified as lost in the MRCAs of the Glomeromycotina, we note the missing key enzymes involved in essential metabolic functions, such as sugar and thiamine metabolisms, or in the biosynthesis of fatty acids. These genes are also referred to as missing glomeromycotina core genes (MGCGs; see table of “Orthogroups lost in the MRCAs of Glomeromycotina” in Data S1; see table of “Missing MRCA genes across glomeromycotina core genes” in Data S1). Our analysis reveals that these have also been lost by *G. pyriformis*. Other key losses found in all sequenced Glomeromycotina include enzymes that actively degrade plant cell wall (see table of “Presence and absence of plant and fungal cell wall related CAZymes” in Data S1). Among the 661 orthogroups gained in the MRCA, most encode for proteins involved in signaling pathways (e.g., protein kinases), protein-protein interactions (e.g., the tetratricopeptide repeat, Sel1, the

Table 1. Summary statistics for genome assembly of sequenced *G. pyriformis* and other species from Glomeromycotina and selected Mucoromycota used in this study

Genomes	Assembly Size	No. of Scaffolds	Scaffold N50	Largest Scaffold (Kb)	Total Gap%	Repeat %	Busco Completeness %	GC %
<i>Geosiphon Pyriformis</i>	129	795	703	2,733.91	0.023	64.35	96.2	29.25
<i>Gigaspora rosea</i> V1.0	597.95	7,526	734	1,204.75	7.92	63.44	97.9	28.81
<i>Rhizophagus ceribriforme</i> DAOM227022 V1.0	136.89	2,592	266	709.02	17.60	24.77	98.3	26.55
<i>Rhizophagus irregularis</i> DAOM 197198V2.0	136.80	1,123	129	1,375.86	5.06	26.38	98	27.53
<i>Diversispora versiformis</i> strain IT104	147	731	434	2,010.39	0.061	43.6	98.2	25.1
<i>Rhizopus microsporus</i> ATCC11559 V1	25.97	131	8	2,782.17	2.41	4.68	98.6	37.48
<i>Mucor Circinelloides</i> CBS 277.49 V2.0	36.59	26	4	6,050.25	0.00	20.38	97.2	42.17
<i>Phycomyces Blakesleeanus</i> NRRL1555 V2.0	53.94	80	11	4,452.46	1.06	9.74	96.9	35.78
<i>Mortierella Elongata</i> AG-77	49.86	473	31	1,526.29	0.30	4.63	99.7	48.05

homodimerization BTB [Broad-Complex, Tramtrack and Bric a brac], and WD-40 domain-containing proteins) and High Mobility Box (HMG) (see table of “Functions of genes which are gained in orthogroups” in [Data S1](#)).

Comparative genomics also showed that *G. pyriformis* carries the same signatures of sexual reproduction found in AMF relatives. These include a complete set of meiosis-specific genes (see table of “Identification of Meiosis specific genes” in [Data S1](#))^{30,31} and a highly conserved genomic locus with architecture and sequence similarity to the mating-type (MAT) locus of basidiomycetes^{22,32,33} (see figure of “Transcriptional directions of the putative AMF mating-type locus” in [Data S1](#)).

Regulation of orthogroups gained in the MRCA of Glomeromycotina

We investigated available gene-expression data from the model AMF *Rhizophagus irregularis* and found that 7 and 39 orthogroups (with a total of 8 and 272 genes; see table of “Upregulation of ortholog genes from Rhiir2 genome” in [Data S1](#) and see table of “Downregulation of Orthogroups genes from Rhiir2” in [Data S1](#)) gained in the MRCA of *Glomeromycotina* are, respectively, upregulated and downregulated across all four experimental conditions in the model AMF *Rhizophagus irregularis*.

These conditions include symbiotic associations between *R. irregularis* and distinct plant hosts (*Medicago truncatula*, *Brachypodium distachyon*)^{34–36} and others based on laser-capture microdissection arbuscule-specific gene expression.^{34,35,37} We investigated the putative function of these differentially regulated genes by identifying protein motifs along their coding sequences and found that these are involved in a myriad of putative cellular functions, which mostly include protein tyrosine kinases, cytochrome p450, as well as FAD binding (see table of “Upregulation of ortholog genes from Rhiir2 genome” and “Downregulation of Orthogroups genes from Rhiir2” in [Data S1](#)). One differentially regulated OG (OG0001728) also shows evidence of originating from horizontal gene transfer from bacteria—i.e., this orthogroup is shared between bacteria and fungi ([Figure S3](#)).

Distinct genomic features of *Geosiphon pyriformis*

The *G. pyriformis* genome also offers an opportunity to identify innovations linked to the emergence of the only known cyanobacteria—fungus endosymbiosis. To identify such innovations, hierarchical clustering of abundance Pfam domains was performed using available genomes in the Glomeromycotina and representatives of Mucoromycotina and Mortierellomycotina ([Figure S4](#)). This analysis revealed a significant overrepresentation of 16 protein domains in *G. pyriformis* compared to relatives in the Mucoromycota—e.g., Lipase_3, RNase_H, Retrotrans gag domains, dUTPase, Spuma_A9PTase, Myb_DNA-bind_6 (see table of “Pfam domain counts from genomes of mucoromycota used in this study” and “p values calculated by Fisher’s test” in [Data S1](#)).

We also sought evidence of horizontal gene transfers (HGTs) between partners of the unique *Geosiphon-Nostoc* endosymbiosis and found 18 genes with potential bacterial within in the *G. pyriformis* genome (see table of “HGT containing genes with pfam domains” in [Data S1](#)). Among putative HGTs, two are protein encoding genes with significant sequence conservation with *Nostoc* or Gamma proteobacteria homologs (see figure of “Phylogenetic tree showing evidence of Horizontal gene transfer of Selenium binding protein” and “Phylogenetic tree showing evidence of horizontal gene transfer in Molybdenum cofactor carrier” in [Data S1](#)). All putative HGTs are located within contigs with average coverage and surrounded by genes of AMF origin, suggesting these do not represent contaminants.

DISCUSSION

MRCA of all extant Glomeromycotina carried the hallmarks of mutualism and obligate biotrophy

Genome data from a representative of the basal node of the AMF phylogeny filled an important gap in understanding the origin of AMS. Specifically, it allowed us to conclude that the MRCA of all extant Glomeromycotina carried the hallmarks of mutualism and obligate biotrophy—i.e., a lack of genes for

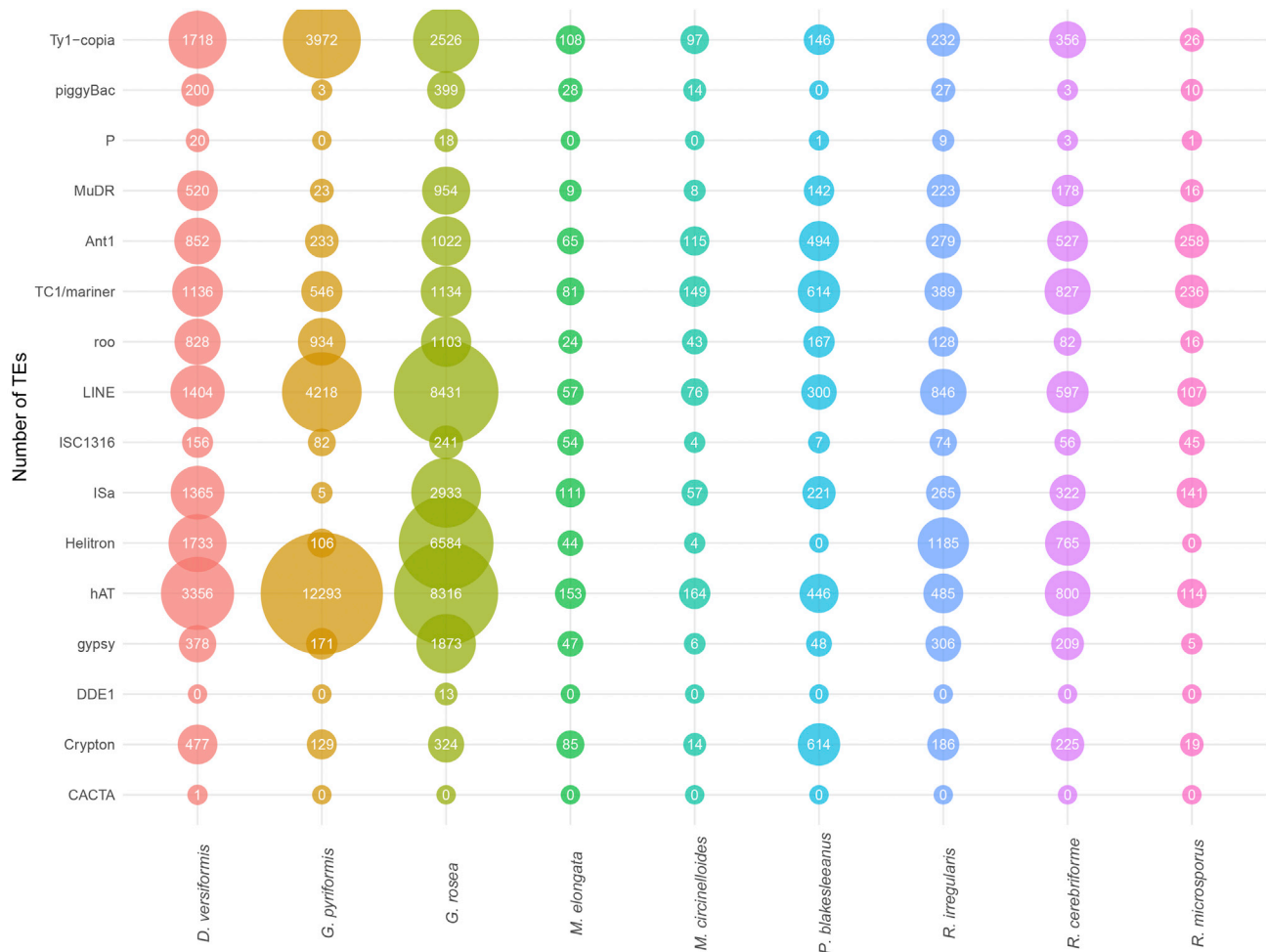


Figure 2. Bubble plot containing all transposable elements in the genomes of glomeromycotina and mucromycotina genomes used in this study

The figure shows the expansion of Gypsy elements in *G. pyriformis*.

fatty acids and thiamine biosynthesis and nutrition and a reduced number of genes that actively degrade plant cell walls. Thus, the mechanisms involved in AMS appeared prior to the emergence of Glomeromycotina and likely represent a synapomorphy of this sub-phyllum. *G. pyriformis* has also conserved genomic signatures of sexual reproduction, as well as an apparent low nuclear polymorphism. Both traits are thus conserved across Glomeromycotina and are in stark contrast with the notion that these organisms represent an ancient asexual lineage.

The retention of a conserved Glomeromycotina gene set in *G. pyriformis*, including a subset of these involved in plant cell wall degradation, indicates that this species might be capable to form mycorrhizae, although this has never been observed. Specifically, this gene set retention could reflect an intrinsic capacity for *G. pyriformis* to undergo classic (but rare) mycorrhizal associations with plants under the right conditions. Although speculative at this point, this hypothesis is supported by the identification of rare *Geosiphon*-like sequences in environmental samples.^{38–40}

Novel symbiotic abilities and horizontal gene transfers in *G. pyriformis*

As a result of losses in fatty acid biosynthesis genes, AMF are entirely dependent on the host plant they associate with to obtain lipids.^{41–44} Within this context, our findings suggest that, during the switch from regular AMS to a fungal-cyanobacteria symbiosis, *G. pyriformis* evolved novel strategies to utilize lipids from its new host through the expansion of specific gene motifs. Specifically, the *G. pyriformis* genome carries a striking over-representation of Lipase 3 protein domains that hydrolyze ester linkages of fatty acids. As *Nostoc* spp is known to produce a wide variety of extracellular lipids in high amounts,^{41–44} it is possible that these abundant lipids are released in the environment (like many other cellular compounds released by cyanobacteria^{45–48}) and are then broken down by lipases to be used as an energy resource by *G. pyriformis*.

As we find evidence of bacteria-like genes in the *G. pyriformis* genome, our work also suggests that the co-existence of multiple endosymbionts and *G. pyriformis* nuclei within restricted

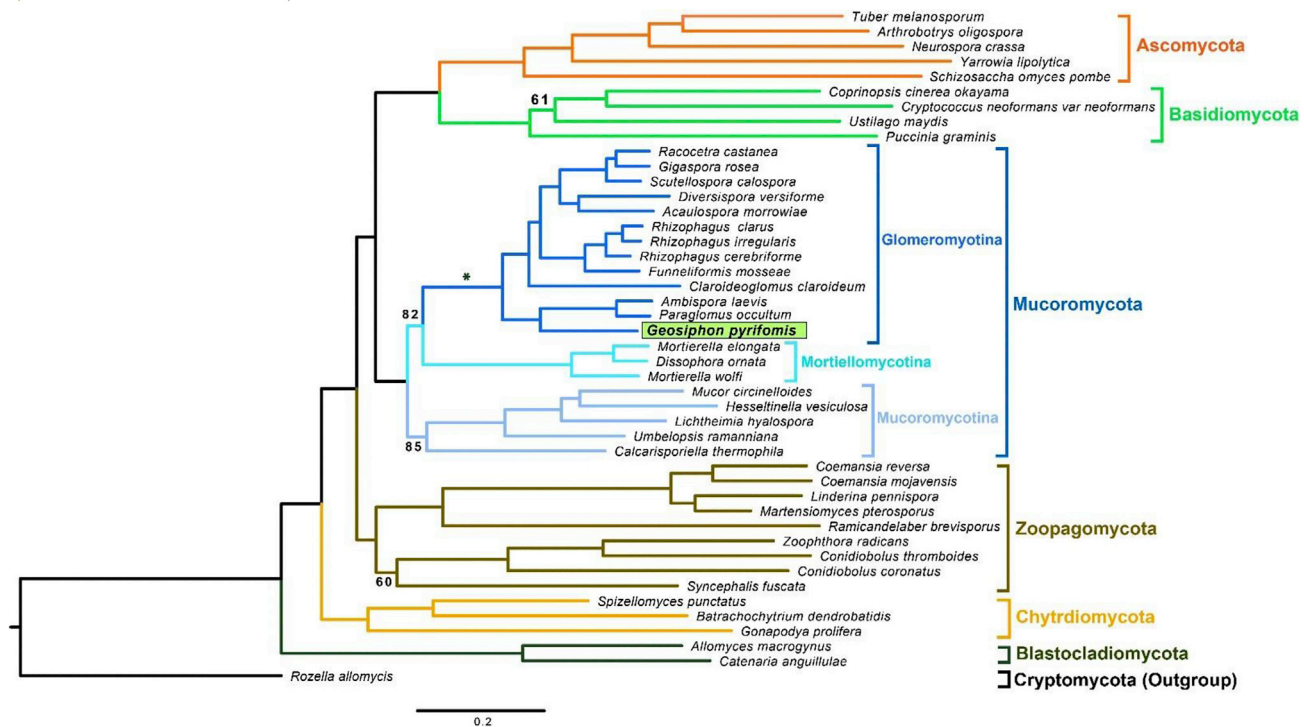


Figure 3. Phylogenetic tree representing the evolutionary relationships of fungi and placement of *G. pyriformis* in Glomeromycotina clade
The tree was resolved using maximum likelihood phylogenetic reconstruction with IQ-TREE on a concatenated alignment of 434 protein coding genes. Numbers indicate nodes with less than 100% bootstrap support. Branches are colored according to their phylum. The asterisk denotes the location where inferred gene losses and gains occurred in the most recent common ancestors (MRCAs) of Glomeromycotina. See also Figure S1.

bladders offers opportunities for horizontal gene exchange. Although none of the putative bacterial genes we identified in *G. pyriformis* are functionally related, there is evidence that one is differentially regulated during AMF symbiosis, supporting the notion that bacteria-like genes can play a major role in fungal evolution.^{15,49}

Identification of a putative AMF core-symbiotic toolkit

The *G. pyriformis* genome also enabled the identification of a putative core AMF symbiotic toolkit conserved in all the sampled Glomeromycotina. This set of genes is differentially regulated in model AMF during symbiotic interactions with different plant hosts, including dicots, monocots, and non-vascular plants, and thus provides a basis for future research on symbiosis-related mechanisms in these plant symbionts. The identification of a core set of gene gains specifically regulated during mycorrhizal symbiosis, and their conservation across the Glomeromycotina phylogeny also provides support for the early emergence of symbiosis-specific gene functions in AMF over 400 million years ago, contemporaneously with the evolution of the first land plants.^{50,51} Last, as genetic transformation is currently infeasible in Glomeromycotina, only assumptions can be proposed for the function of these putative core genes. However, as some encode for chitin synthases, one attractive hypothesis could be that some evolved for the production of short-chain chitooligosaccharides or lipo-chitooligosaccharides that are known symbiotic signals

triggering the activation of the symbiotic program on the host plant.^{2,52,53}

STAR★METHODS

Detailed methods are provided in the online version of this paper and include the following:

- KEY RESOURCES TABLE
- RESOURCE AVAILABILITY
 - Lead contact
 - Materials availability
 - Data and code availability
- EXPERIMENTAL MODEL AND SUBJECT DETAILS
- METHOD DETAILS
 - Cultivation of *G. pyriformis* samples from natural habitat
 - Genome and transcriptome sequencing and assembly
 - Genome annotation
 - SNP calling and allele frequency analysis
 - Phylogenetic analysis and molecular dating
 - Alternative topology test and dating analyses
 - Detection of putative horizontal gene transfers
 - Gene orthology and evolution of symbiotic specific genes
 - Differential expression analysis and combination of expression data to orthogroups
- QUANTIFICATION AND STATISTICAL ANALYSIS

SUPPLEMENTAL INFORMATION

Supplemental Information can be found online at <https://doi.org/10.1016/j.cub.2021.01.058>.

ACKNOWLEDGMENTS

We thank Vasilis Kokkoris and Allison MacLean for comments on an earlier version of the manuscript. N.C.'s research is funded by the discovery program of the Natural Sciences and Engineering Research Council (RGPIN-2020-05643) and the Discovery Accelerator Supplements program (RGPAS-2020-00033). N.C. is a University of Ottawa Research chair in Microbial Genomics. M.K. and C.K. were funded by the Czech Sciences Foundation (GAČR) as a junior grant with the project number GJ16-16406Y. This work was also supported by the Agence Nationale de la Recherche (ANR) grant EVOLSYM (ANR-17-CE20-0006-01) to P.-M.D., by the Bill and Melinda Gates Foundation as Engineering the Nitrogen Symbiosis for Africa (OPP1172165) to P.-M.D., and by Laboratoire de Recherche en Sciences Végétales (LRSV) laboratory, which belongs to the TULIP Laboratoire d'Excellence (ANR-10-LABX-41). J.E.S. is a CIFAR Fellow in the program Fungal Kingdom: Threats and Opportunities. Y.W. and J.E.S. were supported by US National Science Foundation grants DEB-1441715 and DEB-1557110.

AUTHOR CONTRIBUTIONS

M.M.C., M.K., C.K., Y.W., J.E.S., P.M., and N.C. planned and designed the research, wrote the manuscript, and helped with the data analysis. M.M.C. carried out the genome annotation and bioinformatics analysis. Y.W. performed the phylogenetic and molecular dating analysis. E.C.H.C. and G.Y. produced the repeat analysis with M.M.C. J.K. performed the ortholog analysis. C.R. performed the transcriptome analysis. M.V.-L. helped improve the quality of the images. M.K. and C.K. produced the biological materials. N.C. supervised all processes.

DECLARATION OF INTERESTS

The authors declare no competing interests.

Received: August 4, 2020

Revised: November 18, 2020

Accepted: January 18, 2021

Published: February 15, 2021

REFERENCES

1. Spatafora, J.W., Chang, Y., Benny, G.L., Lazarus, K., Smith, M.E., Berbee, M.L., Bonito, G., Corradi, N., Grigoriev, I., Gryganskyi, A., et al. (2016). A phylum-level phylogenetic classification of zygomycete fungi based on genome-scale data. *Mycologia* 108, 1028–1046.
2. Parniske, M. (2008). Arbuscular mycorrhiza: the mother of plant root endosymbioses. *Nat. Rev. Microbiol.* 6, 763–775.
3. Brundrett, M.C. (2009). Mycorrhizal associations and other means of nutrition of vascular plants: Understanding the global diversity of host plants by resolving conflicting information and developing reliable means of diagnosis. *Plant Soil* 320, 37–77.
4. Smith, S., and Read, D. (2008). *Mycorrhizal Symbiosis* (Elsevier).
5. Remy, W., Taylor, T.N., Hass, H., and Kerp, H. (1994). Four hundred-million-year-old vesicular arbuscular mycorrhizae. *Proc. Natl. Acad. Sci. USA* 91, 11841–11843.
6. Strullu-Derrien, C., Selosse, M.A., Kenrick, P., and Martin, F.M. (2018). The origin and evolution of mycorrhizal symbioses: from palaeomycology to phylogenomics. *New Phytol.* 220, 1012–1030.
7. Delaux, P.M., Radhakrishnan, G.V., Jayaraman, D., Cheema, J., Malbreil, M., Volkening, J.D., Sekimoto, H., Nishiyama, T., Melkonian, M., Pokorny, L., et al. (2015). Algal ancestor of land plants was preadapted for symbiosis. *Proc. Natl. Acad. Sci. USA* 112, 13390–13395.
8. Radhakrishnan, G.V., Keller, J., Rich, M.K., Vernié, T., Mbadanga Mbadanga, D.L., Vigneron, N., Cottret, L., Clemente, H.S., Libourel, C., Cheema, J., et al. (2020). An ancestral signalling pathway is conserved in intracellular symbioses-forming plant lineages. *Nat. Plants* 6, 280–289.
9. Beaudet, D., Chen, E.C.H., Mathieu, S., Yildirim, G., Ndikumana, S., Dalpé, Y., Séguin, S., Farinelli, L., Stajich, J.E., and Corradi, N. (2018). Ultra-low input transcriptomics reveal the spore functional content and phylogenetic affiliations of poorly studied arbuscular mycorrhizal fungi. *DNA Res.* 25, 217–227.
10. Gehrig, H., Schüssler, A., and Kluge, M. (1996). *Geosiphon pyriforme*, a fungus forming endocytobiosis with *Nostoc* (cyanobacteria), is an ancestral member of the Glomales: evidence by SSU rRNA analysis. *J. Mol. Evol.* 43, 71–81.
11. Redecker, D., Kodner, R., and Graham, L.E. (2000). Glomalean fungi from the Ordovician. *Science* 289, 1920–1921.
12. Schüßler, A., and Walker, C. (2011). Evolution of the 'plant-symbiotic' fungal phylum. In *Evolution of Fungi and Fungal-Like Organisms*, S. Pöggeler, and J. Wöstemeyer, eds. (Springer-Verlag), pp. 163–185.
13. Schüßler, A., Schnepf, E., Mollenhauer, D., and Kluge, M. (1995). The fungal bladders of the endocyanosis *Geosiphon pyriforme*, a Glomus-related fungus: cell wall permeability indicates a limiting pore radius of only 0.5 nm. *Protoplasma* 185, 131–139.
14. Kluge, M., Mollenhauer, D., Wolf, E., and Schüßler, A. (2002). The *Nostoc-Geosiphon* endocytobiosis. *Cyanobacteria in symbiosis* (Dordrecht: Springer), pp. 19–30.
15. Sun, X., Chen, W., Ivanov, S., MacLean, A.M., Wight, H., Ramaraj, T., Mudge, J., Harrison, M.J., and Fei, Z. (2019). Genome and evolution of the arbuscular mycorrhizal fungus *Diversispora epigaea* (formerly *Glomus versiforme*) and its bacterial endosymbionts. *New Phytol.* 221, 1556–1573.
16. Dobin, A., Davis, C.A., Schlesinger, F., Drenkow, J., Zaleski, C., Jha, S., Batut, P., Chaisson, M., and Gingeras, T.R. (2013). STAR: ultrafast universal RNA-seq aligner. *Bioinformatics* 29, 15–21.
17. Smit, A.F.A., Hubley, R., and Green, P. (2010). RepeatMasker Open-3.0. 1996-2010. *Inst. Syst. Biol.* <http://www.repeatmasker.org/faq.html>.
18. Morin, E., Miyauchi, S., San Clemente, H., Chen, E.C.H., Pelin, A., de la Providencia, I., Ndikumana, S., Beaudet, D., Hainaut, M., Druła, E., et al. (2019). Comparative genomics of *Rhizophagus irregularis*, *R. cerebriforme*, *R. diaphanus* and *Gigaspora rosea* highlights specific genetic features in Glomeromycotina. *New Phytol.* 222, 1584–1598.
19. Tisserant, E., Malbreil, M., Kuo, A., Kohler, A., Symeonidi, A., Balestrini, R., Charron, P., Duensing, N., Frei dit Frey, N., Gianinazzi-Pearson, V., et al. (2013). Genome of an arbuscular mycorrhizal fungus provides insight into the oldest plant symbiosis. *Proc. Natl. Acad. Sci. USA* 110, 20117–20122.
20. Mathieu, S., Cusant, L., Roux, C., and Corradi, N. (2018). Arbuscular mycorrhizal fungi: intraspecific diversity and pangenomes. *New Phytol.* 220, 1129–1134.
21. Chen, E.C.H., Morin, E., Beaudet, D., Noel, J., Yildirim, G., Ndikumana, S., Charron, P., St-Onge, C., Giorgi, J., Krüger, M., et al. (2018). High intraspecific genome diversity in the model arbuscular mycorrhizal symbiont *Rhizophagus irregularis*. *New Phytol.* 220, 1161–1171.
22. Ropars, J., Toro, K.S., Noel, J., Pelin, A., Charron, P., Farinelli, L., Marton, T., Krüger, M., Fuchs, J., Brachmann, A., and Corradi, N. (2016). Evidence for the sexual origin of heterokaryosis in arbuscular mycorrhizal fungi. *Nat. Microbiol.* 1, 16033.
23. Dong, S., Raffaele, S., and Kamoun, S. (2015). The two-speed genomes of filamentous pathogens: waltz with plants. *Curr. Opin. Genet. Dev.* 35, 57–65.
24. Malar C, M., Yuzon, J.D., Das, S., Das, A., Panda, A., Ghosh, S., Tyler, B.M., Kasuga, T., and Tripathy, S. (2019). Haplotype-phased genome assembly of virulent phytophthora ramorum isolate ND886 facilitated by long-read sequencing reveals effector polymorphisms and copy number variation. *Mol. Plant Microbe Interact.* 32, 1047–1060.

25. Vandenkoornhuyse, P., Leyval, C., and Bonnin, I. (2001). High genetic diversity in arbuscular mycorrhizal fungi: evidence for recombination events. *Heredity* 87, 243–253.
26. Chen, E.C.C.H., Mathieu, S., Hoffrichter, A., Sedzielewska-Toro, K., Peart, M., Pelin, A., Ndikumana, S., Ropars, J., Dreissig, S., Fuchs, J., et al. (2018). Single nucleus sequencing reveals evidence of inter-nucleus recombination in arbuscular mycorrhizal fungi. *eLife* 7, 1–17.
27. Croll, D., and Sanders, I.R. (2009). Recombination in *Glomus intraradices*, a supposed ancient asexual arbuscular mycorrhizal fungus. *BMC Evol. Biol.* 9, 13.
28. Krüger, M., Krüger, C., Walker, C., Stockinger, H., and Schüssler, A. (2012). Phylogenetic reference data for systematics and phylotaxonomy of arbuscular mycorrhizal fungi from phylum to species level. *New Phytol.* 193, 970–984.
29. Emms, D.M., and Kelly, S. (2019). OrthoFinder: phylogenetic orthology inference for comparative genomics. *Genome Biol.* 20, 238.
30. Corradi, N., and Lildhar, L. (2012). Meiotic genes in the arbuscular mycorrhizal fungi: What for? *Commun. Integr. Biol.* 5, 187–189.
31. Halary, S., Malik, S.B., Lildhar, L., Slamovits, C.H., Hijri, M., and Corradi, N. (2011). Conserved meiotic machinery in *Glomus* spp., a putatively ancient asexual fungal lineage. *Genome Biol. Evol.* 3, 950–958.
32. Idnurm, A., Walton, F.J., Floyd, A., and Heitman, J. (2008). Identification of the sex genes in an early diverged fungus. *Nature* 457, 193–196.
33. Wong, S., Fares, M.A., Zimmermann, W., Butler, G., and Wolfe, K.H. (2003). Evidence from comparative genomics for a complete sexual cycle in the ‘asexual’ pathogenic yeast *Candida glabrata*. *Genome Biol.* 4, R10.
34. Gaude, N., Bortfeld, S., Duensing, N., Lohse, M., and Krajinski, F. (2012). Arbuscule-containing and non-colonized cortical cells of mycorrhizal roots undergo extensive and specific reprogramming during arbuscular mycorrhizal development. *Plant J.* 69, 510–528.
35. An, J., Zeng, T., Ji, C., de Graaf, S., Zheng, Z., Xiao, T.T., Deng, X., Xiao, S., Bisseling, T., Limpens, E., and Pan, Z. (2019). A *Medicago truncatula* SWEET transporter implicated in arbuscule maintenance during arbuscular mycorrhizal symbiosis. *New Phytol.* 224, 396–408.
36. Zeng, T., Holmer, R., Hontelez, J., Te Lintel-Hekkert, B., Marufu, L., de Zeeuw, T., Wu, F., Schijlen, E., Bisseling, T., and Limpens, E. (2018). Host- and stage-dependent secretome of the arbuscular mycorrhizal fungus *Rhizophagus irregularis*. *Plant J.* 94, 411–425.
37. Fiorilli, V., Catoni, M., Miozzi, L., Novero, M., Accotto, G.P., and Lanfranco, L. (2009). Global and cell-type gene expression profiles in tomato plants colonized by an arbuscular mycorrhizal fungus. *New Phytol.* 184, 975–987.
38. Sheng, M., Chen, X., Zhang, X., Hamel, C., Cui, X., Chen, J., Chen, H., and Tang, M. (2017). Changes in arbuscular mycorrhizal fungal attributes along a chronosequence of black locust (*Robinia pseudoacacia*) plantations can be attributed to the plantation-induced variation in soil properties. *Sci. Total Environ.* 599–600, 273–283.
39. Berruti, A., Demasi, S., Lumini, E., Kobayashi, N., Scariot, V., and Bianciotto, V. (2017). Wild *Camellia japonica* specimens in the Shimane prefecture (Japan) host previously undescribed AMF diversity. *Appl. Soil Ecol.* 115, 10–18.
40. Krüger, C., Kohout, P., Janoušková, M., Püschel, D., Frouz, J., and Rydlová, J. (2017). Plant communities rather than soil properties structure arbuscular mycorrhizal fungal communities along primary succession on a mine spoil. *Front. Microbiol.* 8, 719.
41. Temina, M., Rezankova, H., Rezanka, T., and Dembitsky, V.M. (2007). Diversity of the fatty acids of the *Nostoc* species and their statistical analysis. *Microbiol. Res.* 162, 308–321.
42. Patel, V.K., Sundaram, S., Patel, A.K., and Kalra, A. (2018). Characterization of seven species of cyanobacteria for high-quality biomass production. *Arab. J. Sci. Eng.* 43, 109–121.
43. López-Rosales, A.R., Ancona-Canché, K., Chavarria-Hernandez, J.C., Barahona-Pérez, F., Toledano-Thompson, T., Garduño-Solórzano, G., López-Adrian, S., Canto-Canché, B., Polanco-Lugo, E., and Valdez-Ojeda, R. (2019). Fatty acids, hydrocarbons and terpenes of nanochloropsis and nanochloris isolates with potential for biofuel production. *Energies* 12, 130.
44. Steinhoff, F.S., Karlberg, M., Graeve, M., and Wulff, A. (2014). Cyanobacteria in Scandinavian coastal waters - a potential source for biofuels and fatty acids? *Algal Res.* 5, 42–51.
45. Rich, M.K., Nouri, E., Courty, P.E., and Reinhardt, D. (2017). Diet of arbuscular mycorrhizal fungi: bread and butter? *Trends Plant Sci.* 22, 652–660.
46. Luginbuehl, L.H., Menard, G.N., Kurup, S., Van Erp, H., Radhakrishnan, G.V., Breakspear, A., Oldroyd, G.E.D., and Eastmond, P.J. (2017). Fatty acids in arbuscular mycorrhizal fungi are synthesized by the host plant. *Science* 356, 1175–1178.
47. Cordeiro, R.S., Vaz, I.C.D., Magalhães, S.M.S., and Barbosa, F.A.R. (2017). Effects of nutritional conditions on lipid production by cyanobacteria. *An. Acad. Bras. Cienc.* 89 (Suppl), 2021–2031.
48. Keymer, A., Pimprikar, P., Wewer, V., Huber, C., Brands, M., Bucerius, S.L., Delaux, P.M., Klingl, V., Röpenack-Lahaye, E.V., Wang, T.L., et al. (2017). Lipid transfer from plants to arbuscular mycorrhiza fungi. *eLife* 6, e29107.
49. Torres-Cortés, G., Ghignone, S., Bonfante, P., and Schüßler, A. (2015). Mosaic genome of endobacteria in arbuscular mycorrhizal fungi: Transkingdom gene transfer in an ancient mycoplasma-fungus association. *Proc. Natl. Acad. Sci. USA* 112, 7785–7790.
50. Rensing, S.A. (2018). Great moments in evolution: the conquest of land by plants. *Curr. Opin. Plant Biol.* 42, 49–54.
51. Morris, J.L., Puttick, M.N., Clark, J.W., Edwards, D., Kenrick, P., Pressel, S., Wellman, C.H., Yang, Z., Schneider, H., and Donoghue, P.C.J. (2018). The timescale of early land plant evolution. *Proc. Natl. Acad. Sci. USA* 115, E2274–E2283.
52. Genre, A., Chabaud, M., Balzergue, C., Puech-Pagès, V., Novero, M., Rey, T., Fournier, J., Rochange, S., Bécard, G., Bonfante, P., and Barker, D.G. (2013). Short-chain chitin oligomers from arbuscular mycorrhizal fungi trigger nuclear Ca²⁺ spiking in *Medicago truncatula* roots and their production is enhanced by strigolactone. *New Phytol.* 198, 190–202.
53. Maillet, F., Poinso, V., André, O., Puech-Pagès, V., Haouy, A., Gueunier, M., Cromer, L., Giraudet, D., Formey, D., Niebel, A., et al. (2011). Fungal lipochitooligosaccharide symbiotic signals in arbuscular mycorrhiza. *Nature* 469, 58–63.
54. Altschul, S.F., Gish, W., Miller, W., Myers, E.W., and Lipman, D.J. (1990). Basic local alignment search tool. *J. Mol. Biol.* 215, 403–410.
55. Buchfink, B., Xie, C., and Huson, D.H. (2015). Fast and sensitive protein alignment using DIAMOND. *Nat. Methods* 12, 59–60.
56. Kent, W.J. (2002). BLAT—the BLAST-like alignment tool. *Genome Res.* 12, 656–664.
57. Alneberg, J., Bjarnason, B.S., de Bruijn, I., Schirmer, M., Quick, J., Ijaz, U.Z., Lahti, L., Loman, N.J., Andersson, A.F., and Quince, C. (2014). Binning metagenomic contigs by coverage and composition. *Nat. Methods* 11, 1144–1146.
58. Nurk, S., Meleshko, D., Korobeynikov, A., and Pevzner, P.A. (2017). metaSPAdes: a new versatile metagenomic assembler. *Genome Res.* 27, 824–834.
59. Bolger, A.M., Lohse, M., and Usadel, B. (2014). Trimmomatic: a flexible trimmer for Illumina sequence data. *Bioinformatics* 30, 2114–2120.
60. Marçais, G., and Kingsford, C. (2011). A fast, lock-free approach for efficient parallel counting of occurrences of k-mers. *Bioinformatics* 27, 764–770.
61. Zimin, A.V., Marçais, G., Puiu, D., Roberts, M., Salzberg, S.L., and Yorke, J.A. (2013). The MaSuRCA genome assembler. *Bioinformatics* 29, 2669–2677.
62. Vurture, G.W., Sedlazeck, F.J., Nattestad, M., Underwood, C.J., Fang, H., Gurtowski, J., and Schatz, M.C. (2017). GenomeScope: fast reference-free genome profiling from short reads. *Bioinformatics* 33, 2202–2204.

63. Eddy, S.R. (1996). Hidden Markov Models. *Current Opinion in Structural Biology* 6, 361–365.
64. Finn, R.D., Bateman, A., Clements, J., Coggill, P., Eberhardt, R.Y., Eddy, S.R., Heger, A., Hetherington, K., Holm, L., Mistry, J., et al. (2014). Pfam: the protein families database. *Nucleic Acids Res.* 42, D222–D230.
65. Hass, B. (2010). TransposonPSI: An Application of PSI-Blast to Mine (retro-)transposon ORF Homologies (Broad Institute).
66. Nguyen, L.T., Schmidt, H.A., von Haeseler, A., and Minh, B.Q. (2015). IQ-TREE: a fast and effective stochastic algorithm for estimating maximum-likelihood phylogenies. *Mol. Biol. Evol.* 32, 268–274.
67. Lombard, V., Golaconda Ramulu, H., Drula, E., Coutinho, P.M., and Henrissat, B. (2014). The carbohydrate-active enzymes database (CAZy) in 2013. *Nucleic Acids Res.* 42, D490–D495.
68. Sperschneider, J., Dodds, P.N., Gardiner, D.M., Singh, K.B., and Taylor, J.M. (2018). Improved prediction of fungal effector proteins from secretomes with EffectorP 2.0. *Mol. Plant Pathol.* 19, 2094–2110.
69. Garrison, E., and Marth, G. (2012). Haplotype-based variant detection from short-read sequencing, arXiv, 1207.3907. <https://arxiv.org/abs/1207.3907>.
70. Danecek, P., Auton, A., Abecasis, G., Albers, C.A., Banks, E., DePristo, M.A., Handsaker, R.E., Lunter, G., Marth, G.T., Sherry, S.T., et al.; 1000 Genomes Project Analysis Group (2011). The variant call format and VCFtools. *Bioinformatics* 27, 2156–2158.
71. Simão, F.A., Waterhouse, R.M., Ioannidis, P., Kriventseva, E.V., and Zdobnov, E.M. (2015). BUSCO: assessing genome assembly and annotation completeness with single-copy orthologs. *Bioinformatics* 31, 3210–3212.
72. Li, H., and Durbin, R. (2009). Fast and accurate short read alignment with Burrows-Wheeler transform. *Bioinformatics* 25, 1754–1760.
73. Sanderson, M.J. (2003). r8s: inferring absolute rates of molecular evolution and divergence times in the absence of a molecular clock. *Bioinformatics* 19, 301–302.
74. Edgar, R.C. (2004). MUSCLE: multiple sequence alignment with high accuracy and high throughput. *Nucleic Acids Res.* 32, 1792–1797.
75. Capella-Gutiérrez, S., Silla-Martínez, J.M., and Gabaldón, T. (2009). trimAl: a tool for automated alignment trimming in large-scale phylogenetic analyses. *Bioinformatics* 25, 1972–1973.
76. Letunic, I., and Bork, P. (2007). Interactive Tree Of Life (iTOL): an online tool for phylogenetic tree display and annotation. *Bioinformatics* 23, 127–128.
77. Letunic, I., and Bork, P. (2019). Interactive Tree Of Life (iTOL) v4: recent updates and new developments. *Nucleic Acids Res.* 47 (W1), W256–W259.
78. Robinson, M.D., McCarthy, D.J., and Smyth, G.K. (2010). edgeR: a Bioconductor package for differential expression analysis of digital gene expression data. *Bioinformatics* 26, 139–140.
79. Schüßler, A., and Wolf, E. (2005). *Geosiphon pyriformis*—a glomeromycotan soil fungus forming endosymbiosis with cyanobacteria. In *In Vitro Culture of Mycorrhizas*, S. Declerck, J. André Fortin, and D.-G. Strullu, eds, eds. (Springer), pp. 271–289.
80. Mollenhauer, D., and Mollenhauer, R. (1988). *Geosiphon* cultures ahead. *Endocytobiosis Cell Res.* 5, 69–73.
81. Haas, B.J., Papanicolaou, A., Yassour, M., Grabherr, M., Blood, P.D., Bowden, J., Couger, M.B., Eccles, D., Li, B., Lieber, M., et al. (2013). De novo transcript sequence reconstruction from RNA-seq using the Trinity platform for reference generation and analysis. *Nat. Protoc.* 8, 1494–1512.
82. Smit, A., and Hubley, R. (2013). RepeatModeler (RepeatModeler).
83. Kamel, L., Tang, N., Malbreil, M., San Clemente, H., Le Marquer, M., Roux, C., and Frei Dit Frey, N. (2017). The comparison of expressed candidate secreted proteins from two arbuscular mycorrhizal fungi unravels common and specific molecular tools to invade different host plants. *Front. Plant Sci.* 8, 124.
84. Pellegrin, C., Morin, E., Martin, F.M., and Veneault-Fourrey, C. (2015). Comparative analysis of secretomes from ectomycorrhizal fungi with an emphasis on small-secreted proteins. *Front. Microbiol.* 6, 1278.
85. Grigoriev, I.V., Nordberg, H., Shabalov, I., Aerts, A., Cantor, M., Goodstein, D., Kuo, A., Minovitsky, S., Nikitin, R., Ohm, R.A., et al. (2012). The genome portal of the Department of Energy Joint Genome Institute. *Nucleic Acids Res.* 40, D26–D32.
86. Grigoriev, I.V., Nikitin, R., Haridas, S., Kuo, A., Ohm, R., Otilar, R., Riley, R., Salamov, A., Zhao, X., Korzeniewski, F., et al. (2014). MycoCosm portal: gearing up for 1000 fungal genomes. *Nucleic Acids Res.* 42, D699–D704.
87. Stajich, J.E. (2017). Fungal genomes and insights into the evolution of the kingdom. *Microbiol. Spectr.* 5, 619–633.
88. Lanfear, R., Calcott, B., Ho, S.Y.W., and Guindon, S. (2012). Partitionfinder: combined selection of partitioning schemes and substitution models for phylogenetic analyses. *Mol. Biol. Evol.* 29, 1695–1701.
89. Parfrey, L.W., Lahr, D.J.G., Knoll, A.H., and Katz, L.A. (2011). Estimating the timing of early eukaryotic diversification with multigene molecular clocks. *Proc. Natl. Acad. Sci. USA* 108, 13624–13629.
90. Lutzoni, F., Nowak, M.D., Alfaro, M.E., Reeb, V., Miadlikowska, J., Krug, M., Arnold, A.E., Lewis, L.A., Swofford, D.L., Hibbett, D., et al. (2018). Contemporaneous radiations of fungi and plants linked to symbiosis. *Nat. Commun.* 9, 5451.
91. Wang, Y., White, M.M., and Moncalvo, J.-M.M. (2019). Diversification of the gut fungi Smittium and allies (Harpellales) co-occurred with the origin of complete metamorphosis of their symbiotic insect hosts (lower Diptera). *Mol. Phylogenet. Evol.* 139, 106550.
92. Chang, Y., Wang, S., Sekimoto, S., Aerts, A.L., Choi, C., Clum, A., LaButti, K.M., Lindquist, E.A., Yee Ngan, C., Ohm, R.A., et al. (2015). Phylogenomic analyses indicate that early fungi evolved digesting cell walls of algal ancestors of land plants. *Genome Biol. Evol.* 7, 1590–1601.
93. Langley, C.H., and Fitch, W.M. (1974). An examination of the constancy of the rate of molecular evolution. *J. Mol. Evol.* 3, 161–177.
94. Gill, P.E., Murray, W., and Wright, M.H. (1981). *Practical Optimization* (Academic Press).
95. Press, W.H., Flannery, B.P., Teukolsky, S.A., and Vetterling, W.T. (1992). *Numerical Recipes in C, Second Edition* (Cambridge University Press).
96. Shimodaira, H. (2002). An approximately unbiased test of phylogenetic tree selection. *Syst. Biol.* 51, 492–508.
97. Shimodaira, H., and Hasegawa, M. (1999). Multiple comparisons of log-likelihoods with applications to phylogenetic inference. *Mol. Biol. Evol.* 16, 1114–1116.
98. Kishino, H., Miyata, T., and Hasegawa, M. (1990). Maximum likelihood inference of protein phylogeny and the origin of chloroplasts. *J. Mol. Evol.* 31, 151–160.
99. Kishino, H., and Hasegawa, M. (1989). Evaluation of the maximum likelihood estimate of the evolutionary tree topologies from DNA sequence data, and the branching order in hominoidea. *J. Mol. Evol.* 29, 170–179.
100. Strimmer, K., and Rambaut, A. (2002). Inferring confidence sets of possibly misspecified gene trees. *Proc. Biol. Sci.* 269, 137–142.
101. Kalyaanamoorthy, S., Minh, B.Q., Wong, T.K.F., von Haeseler, A., and Jermini, L.S. (2017). ModelFinder: fast model selection for accurate phylogenetic estimates. *Nat. Methods* 14, 587–589.
102. Wang, Y., White, M.M., Kvist, S., and Moncalvo, J.M. (2016). Genome-wide survey of gut fungi (Harpellales) reveals the first horizontally transferred ubiquitin gene from a mosquito host. *Mol. Biol. Evol.* 33, 2544–2554.
103. Guindon, S., Dufayard, J.F., Lefort, V., Anisimova, M., Hordijk, W., and Gascuel, O. (2010). New algorithms and methods to estimate maximum-likelihood phylogenies: assessing the performance of PhyML 3.0. *Syst. Biol.* 59, 307–321.
104. Camacho, C., Coulouris, G., Avagyan, V., Ma, N., Papadopoulos, J., Bealer, K., and Madden, T.L. (2009). BLAST+: architecture and applications. *BMC Bioinformatics* 10, 421.

STAR★METHODS

KEY RESOURCES TABLE

REAGENT or RESOURCE	SOURCE	IDENTIFIER
Deposited data		
Genome assembly	JAAOMT000000000	https://www.ncbi.nlm.nih.gov/
Genome sequencing reads	SRR11466073	https://www.ncbi.nlm.nih.gov/
Rnaseq reads	SRR12018969, SRR12018968, SRR12018970	https://www.ncbi.nlm.nih.gov/
Bioproject id	PRJNA610605	https://www.ncbi.nlm.nih.gov/
Biosample	SAMN14307302	https://www.ncbi.nlm.nih.gov/
Software and algorithms		
Blast	54,55	https://ftp.ncbi.nih.gov/blast/executables/igblast/release/LATEST/
Blat	56	https://downloads.sourceforge.net/project/blat/Blat%20Full%20Version/32%20bit%20versions/Win2000%20and%20newer/blat3222_32_full.zip?r=&ts=1611605164&use_mirror=managedway
Concoct	57	https://github.com/BinPro/CONCOCT
Spades	58	https://cab.spbu.ru/software/spades/
Trimmomatic	59	http://www.usadellab.org/cms/?page=trimmomatic
Jellyfish	60	https://github.com/gmarcais/Jellyfish
Masurca	61	https://github.com/alekseyzimin/masurca
Funannotate	https://zenodo.org/record/2604804#.X90FMBZ7nIU	https://funannotate.readthedocs.io/en/latest/
Genomescope	62	http://qb.cshl.edu/genomescope/
Diamond blast	55	https://github.com/bbuchfink/diamond
Pfamscan	63,64	https://gist.github.com/olgabot/f65365842e27d2487ad3
TransposonPsi	65	http://transposonpsi.sourceforge.net/
RepeatMasker	17	http://www.repeatmasker.org/
Iqtree	66	http://www.iqtree.org/
Orthofinder	29	https://github.com/davidemms/OrthoFinder
dbCAN	67	http://www.cazy.org/
EffectorP	68	http://effectorp.csiro.au/
Freebayes	69	https://github.com/freebayes/freebayes
Vcftools	70	http://vcftools.sourceforge.net/
Busco	71	https://busco.ezlab.org/
samtools	72	http://www.htslib.org/
R8s	73	https://sourceforge.net/projects/r8s/
Hmmer	63	http://hmmer.org/download.html
Muscle	74	https://2018-03-06-ibioic.readthedocs.io/en/latest/install_muscle.html
TrimAL	75	http://trimal.cgenomics.org/downloads
iTOL	76,77	https://itol.embl.de/upload.cgi
EdgeR	78	https://www.bioconductor.org/packages/release/bioc/html/edgeR.html

RESOURCE AVAILABILITY

Lead contact

Further information and requests for resources and reagents should be directed to and will be fulfilled by the Lead Contact, Nicolas Corradi (ncorradi@uottawa.ca).

Materials availability

This study did not generate new unique reagents.

Data and code availability

Genome assembly is available in NCBI with accession number of JAAOMT000000000 in Genbank. Genome sequencing reads are submitted in SRA with accession number of SRR11466073, Bioproject PRJNA610605, Biosample SAMN14307302 in Genbank. RNA-seq reads are available in SRA with accession of SRR12018969, SRR12018968, SRR12018970 in Genbank. All scripts used to analyze are archived in <https://github.com/madhubioinfo/Geosiphon>.

EXPERIMENTAL MODEL AND SUBJECT DETAILS

AM Fungi *G. pyriformis* were used for this study. Genome assembly is submitted in NCBI accession number of AAOMT000000000.

METHOD DETAILS

Cultivation of *G. pyriformis* samples from natural habitat

G. pyriformis was sampled during autumn in the only known stable habitat near the village Bieber in the Spessart (Germany). Active bladders of the *Geosiphon-Nostoc* endosymbiosis were found in slightly acidic soil (pH 5). The bladders occurred close to the hornwort *Anthoceros* spp. and the liverwort *Blasia pusilla* L., as these plants harbor the cyanobacteria needed to trigger the *Geosiphon-Nostoc* endosymbiosis. After sampling spores and bladders were transferred to the institute in Prühonice and cultured in beakers,^{79,80} which contain a small pot with a sterile mixture of sand and soil (from the original habitat). The cultures were grown in a climate chamber at 18°C with 14 h light and 10 h night. The substrate is kept wet by a filter paper, which reaches from the substrate into a water reservoir in the beaker. To be maintained over time, cyanobacteria be frequently added to the cultures. For our cultures, *Nostoc punctiformis* was obtained from the Culture Collection of Algae (SAG) at the University of Göttingen (Germany) as strain SAG69.79.^{79,80}

Genome and transcriptome sequencing and assembly

High quality DNA was extracted from active bladders of *G. pyriformis* and *Nostoc punctiforme* using the NucleoSpinII Plant kit (Machery-Nagel) and purified with the genomic DNA clean-up kit (Machery-Nagel) using the manufactures recommendations. Total DNA was sent to Fasteris (Switzerland) for library Illumina library preparation and sequencing using on 150 paired end and 5kb mate pairs inserts (illumina Nextera mate pair kit). Sequencing was performed using the Illumina Hiseq 4000 platform. Total RNA was extracted using the RNeasy-Mini Kit (QIAGEN) as per instructions of the manufacturer for library RNA-seq Illumina library preparation with sequencing of 150 cycles and paired ends.

Poor quality and adaptor sequences were trimmed using Trimmomatic⁵⁹ with the following parameters of ILLUMINACLIP:2:30:10 SLIDINGWINDOW:5:20 LEADING:5 TRAILING:5 MINLEN:50. The resulting non-redundant metagenome reads were assembled using metaSPAdes V3.12.0.⁵⁸ Assembled 1 GB of contigs were binned on the basis of tetra nucleotide signature using CONCOCT,⁵⁷ following part of the procedure used to assembly the genome of *Diversispora epigaea*.¹⁵ Binned clusters were annotated using BLAST v 2.6.0+^{54,55} and clusters containing bacterial hits were removed. Using this approach, 21 bona-fide AMF clusters were retained, and used as reference to filter original paired-end and mate pair reads with BLAT v. 36x1.⁵⁶ The reads which had mapped to the filtered contigs and matched by BLAT were then extracted to build cleaned sequence libraries that were assembled with MaSuRCA 3.3.0.⁶¹ Additional round of nr BLAST searches on MaSuRCA assembled contigs were performed to further remove contaminating bacteria. K-mer (k = 21) based methods were used on filtered reads to estimate genome size of *G. pyriformis* using jellyfish 1.1.12⁶⁰ and plotted in GenomeScope 2.0⁶² (see figure of “K-mer distribution of filtered illumina genomic reads of *G. pyriformis*” in [Data S1](#)).

Genome annotation

Protein coding genes were predicted using Funannotate V1.7.4 (<https://funannotate.readthedocs.io/en/latest/>) [<https://doi.org/10.5281/zenodo.3679386>], which automates gene prediction. Assembled transcripts using Trinity⁸¹ and Rnaseq reads mapped bam file were used as transcript evidence for gene call.

Transposable elements were predicted using TransposonPSI.⁶⁵ Repeat sequences were first identified using RepeatModeler⁸² with multiple numbers of iterations. The iteration with the most number of repeats were then used for soft-masking the genome with REPEATMASKER (open 4.0.646).¹⁷ Output files generated from above procedures were used to identify repeat along the assembly. The completeness of genome assembly was assessed with BUSCO version 2.0⁷¹ with default parameters using the fungal gene dataset [fungi_odb9] (see table of “Genome completeness using Busco” in [Data S1](#)).

Putative gene functions were identified using Diamond BLASTX.⁵⁵ Pfam domain analysis were performed using Pfamscan^{63,64} ([Figure S4](#)) (see table “Pfam domain counts from genomes of mucoromycota used in this study” and “pvalues calculated by fisher’s test” in [Data S1](#)) and Carbohydrate-active enzymes (CAZYme) were identified using the dbCAN CAZy database⁶⁷ ([Table S2](#)) (see table of “Presence and absence of plant and fungal cell wall related CAZymes” in [Data S1](#)). Putative CAZymes were further verified through comparisons of data from Morin et al.¹⁸ ([Table S1](#)). Secretory proteins were identified using previously published

pipelines^{83,84} (see table of “Secretome proteins from genomes” in [Data S1](#)), and effectors were identified using EffectorP 2.0⁶⁸ (see table of “effector prediction on *G. Pyriformis* genome” in [Data S1](#)). The putative MAT loci of *Paraglomus* sp., and *R. irregularis* were identified by BLAST search procedures (see figure “Transcriptional directions of the putative AMF mating-type locus” and table “Identification of Meiosis specific genes” in [Data S1](#)). The tests for a two-evolutionary rates analysis was performed in part by measuring intergenic distance among genes in genome using a R script²³ (see figure of “Heatmap showing evidence for a “one speed genome” in *Geosiphon Pyriformis*” in [Data S1](#)). For this study, published genomes of additional Glomeromycotina, Mortierellomycotina, and Mucoromycotina were downloaded from JGI portal MycoCosm database^{85,86} [<https://doi.org/10.1093/nar/gkt1183>].

SNP calling and allele frequency analysis

Filtered Mate Pair and Paired End reads were mapped onto the assembled *G. pyriformis* genome using the BWA-MEM v 0.7.17 algorithm⁷² and sorted into a BAM file using samtools (v 1.9).⁷² Variants were called using FREEBAYES v1.2.0⁶⁹ and filtered using vcftools.⁷⁰ Filtering cutoffs and procedures were as described by in Ropars et al.²² and Morin et al.¹⁸ (see figure “Genome wide allele frequency of *G. Pyriformis* shows it is a homokaryon” in [Data S1](#)). Quality filtered variants and SNPs which passed filtering were used for constructing allele frequency plot using a custom R script (code available in GitHub repository).

Phylogenetic analysis and molecular dating

The phylogenomic analyses employed a set of 434 generally conserved and single-copy proteins in fungi (data available at <https://doi.org/10.5281/zenodo.1413687>), which were developed through efforts of the 1000 fungal genomes project and provided in the Joint Genome Institute MycoCosm site.^{1,86,87} Profile-Hidden-Markov-Models of these markers were searched in the *Geosiphon* predicted protein sequences using HMMER3 (v3.1b2)⁶³ and recovered 393 homologs (out of the 434) in total. The 434 markers in 45 included fungal genomes were further collapsed into 57 partitions using a greedy search embedded in PartitionFinder v.2.1.1 for consistent phylogenetic signals.⁸⁸ Phylogenetic trees were produced using the PHYling pipeline (data available <https://doi.org/10.5281/zenodo.1257002>) and with maximum likelihood method implemented in IQ-TREE (v.1.7-beta9).⁶⁶ Concordance factors across the tree were calculated using the package implemented in IQ-TREE.

The divergence time of *Geosiphon* sp. from the clade of “*Ambispora leptoticha* and *Paraglomus occultum*” was estimated using the R8S v1.81⁷³ with the phylogenetic tree reconstructed from the earlier step. We employed five calibration constraints to calibrate the tree, including the crown groups of Fungi (1100 MYA),⁸⁹ Dikarya (772 MYA),⁸⁹ Chytridiomycota (> 573 MYA),^{90–92} the MRCA of Chytridiomycota and terrestrial fungi (> 750 MYA),^{90–92} and Glomeromycotina (> 460 MYA).¹¹ The divergence time of each clade was inferred using the Langley-Fitch method with Powell algorithm.^{93–95}

Alternative topology test and dating analyses

To test the likelihood of other possible phylogenetic placements of *G. pyriformis*, we first reconstructed the associated phylogenetic trees using constraint tree topology as illustrated in [Figure S2](#) via “-g” option of the IQTREE package (iqtree-1.7-beta9)⁶⁶ (see table “Results of alternative tree topology test for phylogenetic tree” in [Data S1](#)). We then compared our best tree (shown as [Figure 3](#)) with alternative topologies to compute the log-likelihoods of the trees using Kishino-Hasegawa test, Shimodaira-Hasegawa test, expected likelihood weight, and approximately unbiased test via “-zb” and “-au” parameters in IQTREE.^{96–100} All tests were performed with 10,000 resampling estimated log-likelihood (RELL) method for reliable results. The best-fit substitution models for the genome-scale data matrix were estimated using ModelFinder implemented in IQTREE package.¹⁰¹

Detection of putative horizontal gene transfers

To identify genes in *Geosiphon* that have potential origin in cyanobacteria, we compared the *Geosiphon* sp. genome to the available fungal and cyanobacterial genomes. To highlight potential HGT genes, we used a Python script (available in github repository)¹⁰² to filter out genome component in *G. pyriformis* with higher similarity score to cyanobacteria than any fungi, excluding the *G. pyriformis* itself (see figure of “Phylogenetic tree showing evidence of horizontal gene transfer in selenium binding protein” and “Phylogenetic tree showing evidence of horizontal gene transfer in Molybdenum cofactor carrier” in [Data S1](#)) (see table of “HGT containing genes with pfam domains” in [Data S1](#)).

Gene orthology and evolution of symbiotic specific genes

Orthogroups resulting from the OrthoFinder run were parsed using a custom Python script. To be retained, an orthogroup had to fill the following conditions: any sequence from the non-AMS fungi, at least one sequence of *Geosiphon pyriformis*, one sequence of either *Rhizophagus irregularis* or *Rhizophagus cerebriforme* and at least one sequence of *Gigaspora rosea* or *Diversispora epigaea* (see table of “Functions of genes which are gained in orthogroups” in [Data S1](#)). Reciprocally, orthogroups that could correspond to gene losses in the AMS fungi were extracted by retaining orthogroups with no sequences of AMS fungi and at least one sequence of each non-AMF fungi ([Table S3](#)) and (see table of “Orthogroups lost in the MRCA of Glomeromycotina” and “Missing MRCA genes across glomeromycotina core genes” in [Data S1](#)).

Orthogroups showing evidence of regulation in symbiotic conditions in *R. irregularis* were subjected to Maximum Likelihood (ML) analysis^{98,103} to check for the absence of non-AMS species. First, proteins contained in orthogroups were searched against the nine proteomes of 9 distinct species using the BLASTp+ v2.9.0¹⁰⁴ with default parameters and an e-value threshold fixed at 1e-05

(threshold was set to 1e-03 when no non-AMS species sequences were identified). Then, proteins were aligned using MUSCLE v3.8.31⁷⁴ with default parameters and resulting alignment trimmed to remove positions with more than 80% of gaps using trimAl v1.4rev22.⁷⁵ Prior to ML reconstruction, best fitting evolution model was tested using ModelFinder¹⁰¹ and then ML analysis was performed using IQ-TREE v1.6.1⁶⁶ with 10,000 replicates of SH-aLRT. Trees were visualized and annotated with the iTOL platform v5.5^{76,77} (Figure S3).

After first round of phylogeny, orthogroups showing an AMF specific pattern were blasted against the full MycoCosm database (1565 proteomes, last accessed: 03/01/2020) to confirm the AMF-specific pattern and a phylogenetic analysis was performed following the procedure described above.

Differential expression analysis and combination of expression data to orthogroups

Expression data of *Rhizophagus irregularis* in four conditions were used to select orthogroups containing gene significantly deregulated in symbiosis for further analysis. Paired-end reads were trimmed and fragments mapped onto Rhiir2_1 genome assembly of *R. irregularis* (https://mycocosm.jgi.doe.gov/Rhiir2_1/). Stringent settings of mapping were used (similarity and length read mapping criteria at 98% and 95%, respectively). Genes differentially expressed (DEG) *in planta* compared to extraradical mycelium were identified after EdgeR⁷⁸ normalization with a false discovery rate (FDR) correction using CLC Genomic Workbench (QIAGEN). We retained genes showing an expression > 2- or < -2-fold times *in planta* compared to extraradical hyphae (FDR ≤ 0.05). Sets of 2683, 2518 and 2410 DEG were found in *M. truncatula*, *B. distachyon* and *L. cruciata* respectively (see table “Upregulation of ortholog genes from Rhiir2 genome” and “Downregulation of ortholog genes from Rhiir2 genome” in Data S1). Detailed information on the data are available at the National Center for Biotechnology Information (NCBI) Gene Expression Omnibus (GEO) portal (accession no GSE67926). The analysis performed on RNA-seq data from arbuscocytes in *M. truncatula*³⁷ presented 6359 DEG.

QUANTIFICATION AND STATISTICAL ANALYSIS

Statistical analysis and graphs were generated using R studio version 4.0.1 (2020-06-06)